Rotational Resonance Tickling: Accurate Internuclear Distance Measurement in Solids

ARTICLE *in* JOURNAL OF THE AMERICAN CHEMICAL SOCIETY · NOVEMBER 1997

Impact Factor: 12.11 · DOI: 10.1021/ja964313z

3 AUTHORS, INCLUDING:

Robert G Griffin
Massachusetts Institute of Technology
454 PUBLICATIONS **24,502** CITATIONS

Rotational Resonance Tickling: Accurate Internuclear Distance Measurement in Solids

Philip R. Costa, Boqin Sun,† and Robert G. Griffin*

Contribution from the Francis Bitter Magnet Laboratory and Department of Chemistry, Massachusetts Institute of Technology, Cambridge, Massachusetts 02139-4307

Received December 16, 1996. Revised Manuscript Received July 25, 1997[⊗]

Abstract: Accurate distance measurements between pairs of nuclear spins can provide detailed information about molecular structure in the solid state. The rotational resonance (R^2) technique, in particular, has been used to measure internuclear distances in a variety of compounds, often between pairs of ^{13}C nuclei where the outer range is 5−6 Å. Recent studies have revealed that the spin dynamics at rotational resonance are influenced by zero-quantum line shape parameters including T_2^{zq} and the dispersion in isotropic chemical shift differences. Errors in the estimation of these parameters are often the limiting factor in determining the accuracy of a distance measurement. Here we present a modification of R^2, termed "rotational resonance tickling" (R^2T), which uses a ramped rf field to induce fast passage through the dipolar resonance condition, thereby greatly reducing the dependence of the spin dynamics on zero-quantum parameters. Extraction of distance information from the resulting exchange curves is approximately a single-parameter fit, with accuracies in model systems that appear to be on the order of ±0.1 Å or better. An additional feature of the technique is that it does not demand the very high-power ^1H decoupling fields typically required in other recoupling experiments to limit signal loss during mixing. We demonstrate the technique in a pair of $^{13}C_2$-labeled model compounds, tyrosine ethyl ester and glycylglycine hydrochloride, with effective internuclear distances (including intermolecular effects) of 5.05 and 4.3 Å, respectively.

Introduction

The measurement of internuclear distances between nuclear spin pairs in solids has become a relevant and heavily exploited tool for investigating the molecular structure of biological samples including membrane and crystalline proteins[1,2] and peptide aggregates.[3,4] In the usual approach, isotopic labeling of the biomolecule of interest with low-γ nuclei (e.g. ^{13}C, ^{15}N) creates an easily manipulated nuclear spin system where the spatial distribution of the spins is determined by the conformation of the molecule. Nuclear magnetic resonance (NMR) experiments which allow measurement of interspin distances then report directly on molecular structure. These experiments are generally performed within the framework of the CP/MAS technique,[5,6] where cross-polarization (CP)[7] from I spins (generally ^1H nuclei) to the low-γ nuclei (*S* spins) of interest increases the signal-to-noise ratio (S/N). Concurrently, magic-angle spinning (MAS)[8,9] increases S/N and spectral resolution by collapsing the broad powder patterns characteristic of static solids into narrow center bands and a series of flanking side bands spaced at the spinning frequency. High-power proton decoupling (HPPD) is applied after CP, where necessary, to remove the effects of abundant ^1H nuclei on the subsequent spin dynamics.

Because MAS also attenuates the dipolar interactions between low-γ nuclei, which encode information about nuclear proximity, some method of interfering with this attenuation is often necessary to extract structural information. A wide variety of "dipolar recoupling" techniques have been introduced in recent years expressly for this purpose.[10] The majority are based on a simple principle: the spin components of the dipolar interaction can be modulated with rf pulses in a manner that interferes with MAS modulation of the spatial part of the interaction, thereby reintroducing structural information to the spin dynamics. Unfortunately, vigorous rf manipulation of the *S*-spin system often interferes with the high-power ^1H decoupling concurrently applied to most samples, leading to significant *S*-spin signal loss during the experiment.[11,12] This limits the distance range over which such recoupling techniques are useful. The problem is particularly acute for experiments on homonuclear spin pairs, where "control" experiments that allow elimination of the signal loss contribution to the observed dynamics are difficult to define.

The rotational resonance (R^2) recoupling technique[13,14] does not suffer from these signal loss limitations. In the R^2 approach, the sample spinning speed is matched to a (sub)multiple of the isotropic chemical shift difference between a pair of homonuclear spins, so that the chemical shift-induced modulation of the coupling between the spins leads to a recoupling effect that in many cases can be exploited to allow measurement of the

† Present address: Magnetic Resonance Department, Schlumberger-Doll Research Laboratory, 110 Schlumberger Drive, Sugarland, TX 77478.

[⊗] Abstract published in *Advance ACS Abstracts,* September 15, 1997.

(1) Lakshmi, K. V.; Auger, M.; Rapp, J.; Lugtenburg, J.; Griffin, R. G.; Herzfeld, J. *J. Am. Chem. Soc.* **1993**, *115*, 8515.

(2) Christensen, A. M.; Schaefer, J. *Biochemistry* **1993**, *32*, 2868.

(3) Lansbury, P. T., Jr.; Costa, P. R.; Griffiths, J. M.; Simon, E. J.; Auger, M.; Halverson, K. J.; Kocisko, D. A.; Hendsch, Z. S.; Ashburn, T. T.; Spencer, R. G. S.; Tidor, B.; Griffin, R. G. *Nat. Struct. Biol.* **1995**, *2*, 990−998.

(4) Heller, J.; Kolbert, A. C.; Larsen, R.; Ernst, M.; Bekker, T.; Baldwin, M.; Prusiner, S. B.; Pines, A.; Wemmer, D. E. *Protein Sci.* **1996**, *5*, 1655.

(5) Schaefer, J.; Stejskal, E. O. *J. Am. Chem. Soc.* **1976**, *98*, 1030.

(6) Maricq, M. M.; Waugh, J. S. *J. Chem. Phys.* **1979**, *70*, 3300.

(7) Pines, A.; Gibby, M. G.; Waugh, J. S. *J. Chem. Phys.* **1973**, *59*, 569−590.

(8) Andrew, E. R.; Bradbury, A.; Eades, R. G. *Nature* **1958**, *182*, 1659.

(9) Lowe, I. J. *Phys. Rev. Lett.* **1959**, *2*, 285.

(10) Bennett, A. E.; Griffin, R. G.; Vega, S. In *NMR Basic Principles and Progress*; Diehl, P., Fluck, E., Gunther, H., Kosfeld, R., Seelig, J., Eds.; Springer-Verlag: Berlin, 1994; Vol. 33, pp 1−77.

(11) Ishii, Y.; Ashida, J.; Terao, T. *Chem. Phys. Lett.* **1995**, *246*, 439−445.

(12) Bennett, A. E. Thesis, MIT, 1995.

(13) Raleigh, D. P.; Levitt, M. H.; Griffin, R. G. *Chem. Phys. Lett.* **1988**, *146*, 71−76.

(14) Levitt, M. H.; Raleigh, D. P.; Creuzet, F.; Griffin, R. G. *J. Chem. Phys.* **1990**, *92*, 6347−6364.

S0002-7863(96)04313-2 CCC: $14.00

internuclear distance. This limits application of the technique to spin pairs with significant isotropic chemical shift differences. However, because no rf manipulation of the spin system is required (beyond encoding and decoding the appropriate initial and final conditions, respectively), essentially no rf-dependent signal loss occurs, and the experiment is sensitive to dipolar couplings corresponding to internuclear $^{13}C-^{13}C$ distances up to 5−6 Å.[15]

It is well-known that the magnetization exchange curves obtained using the R^2 technique (and from which distance information is extracted) are sensitive to parameters in addition to the internuclear distance. In particular, the zero-quantum homogeneous line width parameter T_2^{zq} [14] and the inhomogeneous zero-quantum line shape (of relevance in systems with resonances broadened by chemical shift dispersion (CSD)[3]) both influence the magnetization exchange trajectory. The accuracy with which these parameters are determined often limits the accuracy of R^2 distance measurements. Although zero-quantum filtering experiments have been proposed that allow direct measurement of the appropriate parameters,[16] these experiments are not directly applicable to the weakly coupled spin systems which are generally of interest. Alternatively, zero-quantum parameters may be estimated from single-quantum measurements, although this alternative involves assumptions about correlation between the sites.[3,17] Using the single-quantum estimation method, it has been suggested that the uncertainties in distance measurements approach 1 Å for $^{13}C-^{13}C$ pairs.[4] We have developed alternative methods for directly determining zero-quantum line shape parameters by studying R^2 exchange dynamics as a function of resonance mismatch; our results do not indicate that the observed errors are of this size.[18] Nevertheless, techniques that attenuate or simply remove the dependence of the exchange dynamics on T_2^{zq} and CSD parameters would provide an improved approach.

Here we propose and demonstrate the effectiveness of "rotational resonance tickling" (R^2T) to circumvent these problems—low-γ signal loss due to interference with ^1H decoupling and exchange dynamics dependent on T_2^{zq} and CSD. R^2T involves spinning slightly faster than the standard $n = 1$ rotational resonance condition and simultaneously applying a relatively weak rf field to the homonuclear spin pair to induce dipole-driven dynamics. Under the appropriate conditions, these dynamics show markedly reduced dependence on both homogeneous and inhomogeneous zero-quantum line shape parameters, with the result that distance information of increased accuracy can be extracted. The resonance phenomenon that underlies this technique is identical to that exploited in other experiments, including the well-known heteronuclear CP experiment under "fast-spinning" conditions,[19,20] and also to variants of the heteronuclear rotary resonance experiment.[21] Homonuclear examples include the work of Nielsen and co-workers,[22] who recently suggested the application of rf fields to systems with small chemical shift differences to induce a homonuclear rotary resonant (HORROR) effect, and Takegoshi *et al.*,[23] who suggested similar experiments and pointed out their connection to standard rotational resonance.

Experimental Methods

$^{13}C_2$-Labeled Samples. Synthesis and purification of $^{13}C_2$-labeled tyrosine ethyl ester (TEE) have been described previously.[15] The ^{13}C labels were placed at the 4′ (OH) carbon of the tyrosyl ring and the methylene carbon of the ethyl moiety. The sample consisted of labeled material diluted 1:10 in unlabeled (natural abundance) TEE, as confirmed by comparison of the intensities of labeled and unlabeled peaks in a series of CP/MAS spectra. Synthesis and purification of $^{13}C_2$-labeled glycylglycine hydrochloride (GG-HCl) have also been described.[24] The ^{13}C labels were placed at the α-carbon of the N-terminal residue and the terminal carboxyl carbon. The labeled material was diluted 1:10 in unlabeled GG-HCl for the NMR experiments.

NMR Experiments. NMR spectra were recorded at 9.4 T (100 MHz ^{13}C) using a custom-designed spectrometer and data acquisition and processing software courtesy of D. Ruben. The custom-designed transmission line probe, courtesy of C. Rienstra, was equipped with a 4 mm Chemagnetics spinning assembly and was more than adequate to achieve the spinning speeds (up to 10−13 kHz) and ^1H and ^{13}C rf fields (40−80 and 1−50 kHz, respectively) used in the experiments. Spinning speeds were locked to within ±2 Hz of the reported values using a Doty spinning speed controller. Samples were packed to fill the entire rotor (a measurement of the rf homogeneity across the sample is discussed below). Recycle delays of 3 s were used in all experiments.

For the R^2T experiments, the $^{13}C_2$-labeled samples were spun about the magic angle at a frequency slightly higher than dictated by the n = 1 rotational resonance condition (typically by a margin on the order of 5%), and a weak rf field was applied to scale the effective field magnitudes to match the generalized resonance condition (discussed in more detail below):

$$\omega_\Sigma \equiv \omega_I^e + \omega_S^e = \omega_r \tag{1a}$$

where the effective field strengths are given by

$$\omega_{I,S}^e = \sqrt{\omega_1^2 + \omega_{I,S}^2} \tag{1b}$$

and ω_1 represents the rf field strength and ω_{IS} represents the appropriate resonance offset. The TEE sample, for example, with a 9.4 kHz chemical shift difference and a 9.9 kHz spinning speed, required an rf field strength of approximately 1.6 kHz (carrier frequency placed in the middle of the two ^{13}C resonances) to match the generalized resonance condition.

The R^2 effect is often exploited within the framework of a longitudinal mixing experiment to observe dipole-driven polarization transfer within a spin pair, analysis of which yields information about the internuclear distance.[13] An obvious modification is required—application of weak CW rf of the appropriate magnitude on the low-γ channel during the dipolar mixing period—to perform the R^2T experiment. Further modification is required to compensate for the fact that the effective fields no longer lie along the rotating frame z-axis. The resulting R^2T pulse sequence for near-longitudinal mixing is diagrammed in Figure 1. After CP from ^1H nuclei (1−2 ms duration), high-power CW decoupling is applied to the ^1H channel for the remainder of the experiment. An optional transverse evolution period follows CP on the S-spin channel (in this case, ^{13}C) to allow for selective inversion of one of the two resonances, followed by application of a 90° pulse to create longitudinal difference polarization (^{13}C carrier placed in the middle of the two resonances for this and subsequent pulses). This sequence is formally identical to a $n = 2$ DANTE[25] sequence, where the CP process accomplishes the purpose of the initial

(15) Raleigh, D. P.; Creuzet, F.; Das Gupta, S. K.; Levitt, M. H.; Griffin, R. G. *J. Am. Chem. Soc.* **1989**, *111*, 4502−4503.
(16) Tomita, Y.; McDermott, A., personal communication.
(17) Heller, J.; Larsen, R.; Ernst, M.; Kolbert, A. C.; Baldwin, M.; Prusiner, S. B.; Wemmer, D. E.; Pines, A. *Chem. Phys. Lett.* **1996**, *251*, 223.
(18) Costa, P. R.; Sun, B. Q.; Griffin, R. G., in preparation.
(19) Stejskal, E. O.; Schaefer, J.; Waugh, J. S. *J. Magn. Reson.* **1977**, *28*, 105.
(20) Meier, B. H. *Chem. Phys. Lett.* **1992**, *188*, 201−207.
(21) Levitt, M. H.; Oas, T. G; Griffin, R. G. *Isr. J. Chem.* **1988**, *28*, 271.
(22) Nielsen, N. C.; Bildsoe, H.; Jakobsen, H. J. *J. Chem. Phys.* **1994**, *101*, 1805−1812.
(23) Takegoshi, K.; Nomura, K.; Terao, T. *Chem. Phys. Lett.* **1995**, *232*, 424.
(24) Halverson, K. J. Thesis, MIT, 1991.
(25) Morris, G. A.; Freeman, R. *J. Magn. Reson.* **1977**, *29*, 433−462.

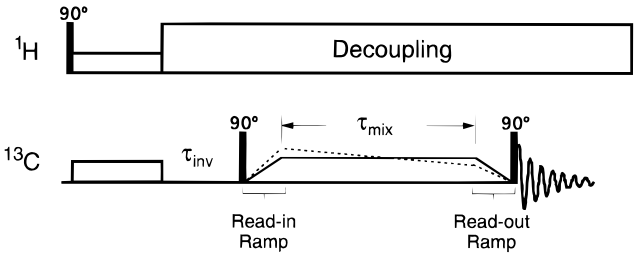

Figure 1. Rotational resonance tickling (R^2T) pulse sequence.

90° DANTE pulse. Omitting the transverse evolution period allows creation of longitudinal sum polarization for control experiments (see below).

Following storage of the magnetization along the *z*-axis of the rotating frame, an adiabatic "ramp-in" (RI) pulse is applied to rotate it to the appropriate near-longitudinal axis for mixing.[26] The magnitude of the rf during this pulse is linearly stepped (in 20−30 increments) from zero to the appropriate magnitude for dipolar mixing, with step duration on the order of 10−30 μs. A complementary "ramp-out" (RO) pulse (with similar step number and duration) is applied at the end of the mixing period to return the magnetization to the rotating frame *z*-axis. The ramp rate for each of these pulses is sufficiently slow to allow for quasi-adiabatic manipulation of the polarization within the rotating frame, while simultaneously being rapid enough to avoid inducing significant dipole-driven dynamics in the weakly coupled spin systems examined here. This is particularly relevant in R^2T experiments where either the RI or the RO pulse passes through a dipolar resonance condition in the course of rotating the polarization within the rotating frame. In more strongly coupled systems, faster RI and RO ramp rates may be necessary to achieve this end.

Between the RI and RO pulses, rf is applied to match resonance and induce dipole-driven dynamics. Setting the rf magnitude to the resonance value during this period will induce R^2-like exchange dynamics, with the expected dependence on chemical shift dispersion and zero-quantum relaxation, and additional dependence on the nature of the rf distribution within the coil. As we show below, however, appropriately ramping the rf amplitude such that the system passes through dipolar resonance induces dipole-driven dynamics which remain a strong function of the dipolar coupling constant but have much reduced dependence on the inhomogeneous (chemical shift dispersion and rf inhomogeneity) and homogeneous (zero-quantum relaxation) effects that limit the accuracy of the standard R^2 experiment. This was achieved in the experiments detailed here by linearly stepping the rf amplitude during the dipolar mixing period through 100 increments spanning the appropriate ramp range (ranges varied and are listed for each case below). The duration of each step was varied from 0.01 to 1 ms (for overall mixing times from 1 to 100 ms). This yielded exchange curves that map out the evolution of sum or difference polarization as a function of ramp rate.

Following the RO pulse, a 90° pulse is applied to create transverse magnetization for detection. The FIDs for each mixing time are processed, and residual sum or difference polarization after mixing is calculated from integrated peak intensities.

Low-power rf field strengths (for the RI/RO and dipolar mixing periods) were measured by the standard nutation method[27] using the R^2T pulse sequence in Figure (1), with the transverse evolution, RI, and RO periods omitted, and the mixing rf phase perpendicular to the ^{13}C CP rf. In these experiments, the ^{13}C carrier frequency was set near the low-field peak in each two-spin sample (within 0.1 kHz) to reduce the CSA-dependent shift and broadening of the nuclear spin precession frequency about the applied rf.[28] FIDs were obtained as a function of the mixing time at constant rf field strength, with dwell time on the order of 100 μs. 2D Fourier transformation of the resulting data set yields an indirect dimension where the near-resonance peak is at the rf nutation frequency. A series of five to eight rf field strengths spanning the low-power regime (1−3 kHz) were measured in this manner, and a linear fit to the data was used to determine the relationship between input rf power and the resulting rf field strength in the coil. An example of the rf distribution across the coil (modified by CP excitation efficiency) is given below.

Numerical Simulation of Spin Dynamics. The simulated exchange curves shown in the following sections were calculated by numerical integration of the equations of motion[29] according to

$$\rho(t + \Delta t) = e^{-iH\Delta t}\rho(t)e^{iH\Delta t} \tag{2}$$

where $\rho(t)$ is the density matrix representing the state of the system at time t, H is the full two-spin Hamiltonian in the rotating frame (see below), and integration time steps were on the order of 1−3 μs. Because the ramped nature of the rf magnitude during mixing rendered the Hamiltonian noncyclic even over successive rotor cycles, stepping through the entire evolution period in this manner was required. Furthermore, each point in the calculated ramp curves required a separate simulation, because these points do not correspond to successive values of an observable along a single mixing period—the ramp rate is different for each. Calculations were performed for a series of randomly selected crystallite orientations (typically on the order of 500−1000), with the results averaged to create the final curve. The values of the terms in the Hamiltonian were determined as follows: (i) the dipolar coupling constant was set as described for each simulation; (ii) CSA tensor elements were derived from the standard Herzfeld−Berger analysis of the side band patterns in slow-spinning spectra,[30] and (iii) relative tensor orientations were ignored, except where otherwise stated.

For simulations including relaxation of 2-quantum coherence, each step of coherent evolution (described by eq 2) was followed by a relaxation step in which the magnitudes of the density matrix elements corresponding to 2-quantum coherence (e.g., $|m_1m_2\rangle\langle m_1',m_2'|$ coherences ($m_i = \pm 1$), where $m_1m_1' + m_2m_2' = -2$) were damped according to the appropriate relaxation rate:

$$[\rho(t + \Delta t)]^+_{ij} = e^{-R\Delta t}[\rho(t + \Delta t)]^-_{ij} \tag{3}$$

where R represents the 2-quantum relaxation rate, the $-$ and $+$ superscripts refer to pre- and postrelaxation, and the (i,j) indices are selected for each 2-quantum matrix element. Because R^2T dynamics occur in a slightly tilted frame (relative to the rotating frame) this simulation method (relaxation in the "Zeeman" basis) does not fully relax the two-spin coherences created during the polarization transfer process. The tilts from the rotating frame are relatively small, however, and since the agreement of our simulation with experiment is excellent, we believe that this is a minor (and hence acceptable) approximation.

Background

Generalized Resonance Condition. The Hamiltonian (in the rotating frame) for a homonuclear spin pair (I and S) evolving under the combined effects of MAS and a weak rf field is:[31]

$$H = \omega_I I_Z + \omega_S S_Z + \omega_1(I_X + S_X) + H_{IS}(t) \tag{4a}$$

where

$$H_{IS} = \omega_D(t)(3I_ZS_Z - \tilde{I}\cdot\tilde{S}) \tag{4b}$$

and

$$\omega_D(t) = \sum_{m=-2}^{2} \omega_D^{(m)} e^{im\omega_r t} \tag{4c}$$

(26) Desvaux, H.; Berthault, P.; Birlirakis, N.; Goldman, M.; Piotto, M. *J. Magn. Reson. A* **1995**, *113*, 47−52.
(27) Bax, A. *Two-Dimensional Nuclear Magnetic Resonance in Liquids*; Delft University Press: Dordrecht, Holland, 1980.
(28) Costa, P. R.; Sun, B. Q.; Griffin, R. G., in preparation.
(29) Abragam, A. *The Principles of Nuclear Magnetism*; Oxford University Press, Inc.: Oxford, UK, 1961.
(30) Herzfeld, J.; Berger, A. E. *J. Chem. Phys.* **1980**, *73*, 6021−6030.
(31) Mehring, M. *Principles of High Resolution NMR in Solids*; Springer-Verlag: Berlin, 1983.

expresses the time dependence imposed on the dipolar couplings by MAS (chemical shifts are assumed to be isotropic). Transformation to a doubly tilted frame in which the effective field for each spin lies along a positive *z*-axis will prove convenient for subsequent calculations and results in a modified Hamiltonian of the form

$$U_T H U_T^{-1} = \omega_I^e I_Z + \omega_S^e S_Z + H_{IS}^T \tag{5a}$$

with $\omega_{I,S}^e = (\omega_1^2 + \omega_{I,S}^2)^{1/2}$, where the tilting transformation is given by

$$U_T = e^{i(\theta_I I_Y + \theta_S S_Y)} \tag{5b}$$

and

$$\theta_{I,S} = \tan^{-1}(\omega_1/\omega_{I,S}) \tag{5c}$$

The tilted dipolar Hamiltonian term is calculated by first expressing its spin part as a product of first-rank, I and S single-spin tensors

$$(3I_Z S_Z - \tilde{I}\cdot\tilde{S}) = T_{20} = 3(T_{10}^{(I)} T_{10}^{(S)}) - \sum_{m=-1}^{1} (-1)^m T_{1m}^{(I)} T_{1-m}^{(S)} \tag{6a}$$

with

$$T_{10} = I_Z, \qquad T_{1\pm1} = \frac{\mp 1}{\sqrt{2}} I_\pm \tag{6b}$$

so that the tilted term is

$$H_{IS}^T = \sum_{m=-2}^{2} \omega_D^{(m)} e^{im\omega_r t} \sum_{m',m''=-1}^{1} C_{m',m''} T_{1m'}^{(I)} T_{1m''}^{(S)} \tag{6c}$$

and

$$C_{m',m''}(\theta_I,\theta_S) = 3d_{0m'}^1(\theta_I) d_{0m''}^1(\theta_S) - \sum_{m'''=-1}^{1} (-1)^{m'''} d_{m''',m'}^1(\theta_I) d_{-m''',m''}^1(\theta_S) \tag{6d}$$

where $d_{m,m'}^1(\theta)$ is the first-rank reduced Wigner matrix.[33]

For couplings that are small compared to the spinning speed ($\omega_r >> |\omega_D^{(m)}|$), the sinusoidal oscillation imposed by MAS on the magnitude of the various components of the coupling is expected to average their effects on the spin dynamics to zero over the course of each rotor period. In the parlance of Average Hamiltonian Theory (AHT),[34,35] the zero-order term in the standard AHT expansion vanishes. Because of the noncommutation of the dipolar and effective field terms in the Hamiltonian, however, higher-order terms in the AHT expansion may be significant, particularly when the size of the effective fields approaches the spinning frequency. Transforming to an interaction frame defined by components of the effective fields reduces their size and so makes the average Hamiltonian calculated in the new frame a valid approximation.

The form of the interaction frame transformation is given by

$$U_I = e^{i(a\omega_r I_Z + b\omega_r S_Z)t/2} \tag{7}$$

where *a* and *b* are integers selected to appropriately minimize the residual effective field terms in the transformed Hamiltonian. We can divide the dipolar terms in eq 6b according to the manner in which they are modulated by this transformation: double-quantum terms modulated at the sum of the I and S transformation frequencies, zero-quantum terms modulated at the difference, antiphase I and S terms modulated at the I or S frequency, and a term that is not modulated.[23] Although all but the last term can in principle be recoupled under appropriate conditions, dominant CSA interactions preclude use of the antiphase terms, and a symmetrically placed carrier yields a difference frequency that is zero and precludes use of the zero-quantum term. Here we focus on the double-quantum term which is responsible for both the $n = 1$ R^2 and HORROR recoupling effects. Under typical conditions the relevant terms in the interaction-frame Hamiltonian will have the form

$$H^{int} = (\omega_\Sigma - \omega_r)(J_Z^{(1,4)}) + C_{11}\omega_D(t)(J_X^{(1,4)} \cos(\omega_r t) + J_Y^{(1,4)} \sin(\omega_r t)) \tag{8}$$

where $\omega_\Sigma = \omega_I^e + \omega_S^e$ and we have used a fictitious spin operator J for the two-level system defined by the double-quantum states $|1\rangle = |{+}{+}\rangle, |4\rangle = |{-}{-}\rangle$.[36,37] Averaging over a rotor cycle, the space and spin modulations of the dipolar term interfere and yield an average Hamiltonian with partial dipolar character:

$$\bar{H}^{int} = (\omega_\Sigma - \omega_r) J_Z^{(1,4)} + C_{11} \frac{b_{IS}}{2\sqrt{2}} \sin 2\beta (J_X^{(1,4)} \cos(\gamma) + J_Y^{(1,4)} \sin(\gamma)) \tag{9a}$$

where the angles β and γ define the dipolar orientation relative to the spinning axis in the standard manner,[38] and the dipolar coupling constant is given by

$$b_{IS} = \left(\frac{\mu_0 \hbar}{2}\right) \frac{\gamma_N^2}{r^3} \tag{9b}$$

When the resonance condition

$$\omega_\Sigma = \omega_I^e + \omega_S^e = \omega_r \tag{10}$$

is precisely matched, the first term vanishes from eq 9a and the average Hamiltonian is purely dipolar. This is the resonant recoupling effect, common to a series of experiments including heteronuclear CP under fast-spinning conditions,[20] standard $R^{2,14}$ and 2Q-HORROR.[22,23] Measurement of the spin dynamics on resonance provides information about the nature of the dipolar interaction. We note that the recoupled Hamiltonian that we have just derived has double quantum character, independent of effective field orientation. It differs from the more familiar zero-quantum R^2 average Hamiltonian in the untilted rotating frame by the 180° rotation of one spin's *z*-axis that connects the untilted rotating frame to the tilted frame appropriate for R^2 in our formalism.

"Longitudinal" Exchange Dynamics. The recoupling effect evident in the average Hamiltonian (eq 9a) is often exploited in the framework of a longitudinal mixing experiment to observe

(32) Reference deleted in proof.
(33) Sakurai, J. J. *Modern Quantum Mechanics*; Addison-Wesley Publishing Co., Inc.: Redwood City, CA, 1985.
(34) Waugh, J. S.; Haeberlen, U. *Phys. Rev.* **1968**, *175*, 453−467.
(35) Haeberlen, U. *High Resolution NMR in Solids*; Academic Press: New York, 1976.
(36) Wokaun, A.; Ernst, R. R. *J. Chem. Phys.* **1977**, *67*, 1752.
(37) Vega, S. *J. Chem. Phys.* **1978**, *68*, 5518.
(38) Spiess, H. W. In *Dynamic NMR Spectroscopy*; Diehl, P., Fluck, E., Kosfeld, R., Eds.; Springer-Verlag: Berlin, 1978; Vol. 15, pp 58−214.

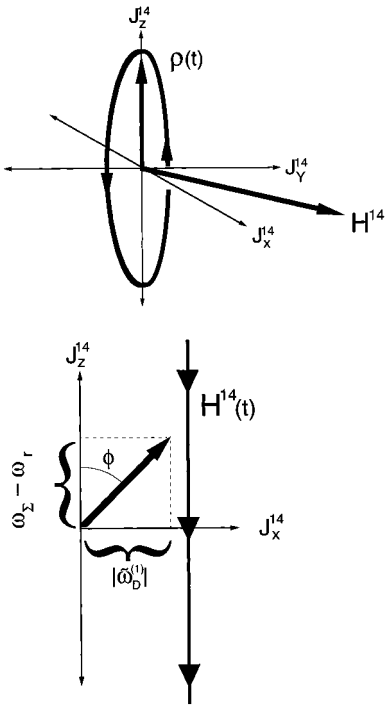

Figure 2. Diagram of spin dynamics in the fictitious *J*-spin frame. (A) On-resonance dynamics, indicating rotation of the vector representing the density matrix about the vector representing the recoupled dipolar Hamiltonian. (B) Ramp-through dynamics, indicating the rotation the Hamiltonian vector undergoes as the effective fields are ramped through resonance. Performed slowly enough, the density matrix will follow the Hamiltonian (corresponding to adiabatic manipulation of the system). In (B), the dipolar component of the Hamiltonian is assumed to lie along the *x*-axis of *J*-space.

dipole-driven spin dynamics in weakly coupled spin pairs.[13,39] Polarization is prepared along the effective fields, and during subsequent mixing on-resonance, dipole-driven spin flips along the effective fields lead to polarization transfer between the coupled sites. The coherent, on-resonance evolution of effective field-locked sum polarization as a function of mixing time (and in a single crystallite) is given by

$$\rho(t) = J_Z^{(1,4)} \cos(|\tilde{\omega}_D^{(1)}|t) + (J_X^{(1,4)} \sin\gamma - J_Y^{(1,4)} \cos\gamma) \sin(|\tilde{\omega}_D^{(1)}|t) \quad (11a)$$

where $\rho(t = 0) = I_Z + S_Z$ represents the initial condition and

$$|\tilde{\omega}_D^{(1)}| = C_{11} \frac{b_{IS}}{2\sqrt{2}} \sin(2\beta) \quad (11b)$$

represents the magnitude of the recoupled dipolar interaction. This describes an oscillation of the density matrix between sum polarization and double-quantum coherence (at a frequency related to the dipolar coupling constant) and is illustrated in the fictitious subspace corresponding to the *J* spin in Figure 2A. In a powder sample, the observed dynamics are an average over all orientations and an inhomogeneously damped oscillation results. Given an ideal case that follows this evolution precisely, the dipolar coupling constant can be extracted directly from analysis of the time-dependent oscillations in the exchange curve.

Relaxation modifies the coherent dynamics in a manner that is particularly complex for weakly coupled systems.[14] In *J*-space, relaxation is often anisotropic: the "transverse" 2-quantum coherence that is created during the polarization transfer process typically has a relaxation time on the order of 1−10 ms, while effective field-locked "longitudinal" polarization may experience little or no relaxation over time scales approaching 1−10 s (this is particularly true when the effective fields in the rotating frame are near longitudinal). For spin pairs in which the recoupled dipolar interaction has a magnitude similar to or smaller than the 2-quantum relaxation rate, the coherent oscillations are damped and a monotonic decay of difference polarization is observed. The details of the decay as a function of mixing time depend strongly on the relative sizes of the 2-quantum relaxation rate and the dipolar coupling constant. Hence an accurate estimate of the 2-quantum relaxation rate is necessary for precise determination of the internuclear distance.[15] A similar dependence of the dipole-driven dynamics on the relevant 2-quantum relaxation rate in weakly coupled systems has been identified in RFDR experiments[12] and is expected for most other homonuclear dipolar recoupling techniques when employed in longitudinal mixing experiments.

A second modification to the exchange dynamics, particular to rotational resonance, arises from CSD. Even in crystalline samples composed of molecules in a single conformation, there is a distribution in the isotropic chemical shift associated with each site. This distribution is attributed to variations in intermolecular packing across the sample which are static, at least on the NMR time scale.[40] Because the distribution in chemical shifts at each site translates into a distribution of isotropic chemical shift differences, it becomes impossible to precisely match the appropriate R^2 condition for all spin pairs in the sample. The exchange dynamics observed by placing the spinning speed at the approximate center of the difference distribution (for the $n = 1$ rotational resonance) are modified according to the nature of the CSD broadening, the modification becoming significant when the width of the distribution is comparable to (or exceeds) the magnitude of the recoupled dipolar interaction.[3,17] This effect also damps the coherent dynamics, in a manner that depends on the size and shape of the broadened resonance condition, and accurate distance measurements require precise quantitation of the CSD contribution to the observed dynamics.

Ramping through Resonance. Application of an rf field of fixed magnitude to perform the R^2T equivalent of an on-resonance longitudinal mixing experiment would exacerbate the problem of extracting an accurate distance since the effects of rf inhomogeneity add to those of CSD. The benefit of the R^2T technique rests instead on the control over matching the resonance condition on short (micro- to millisecond) time scales that an rf component of the effective fields affords. Instead of remaining at the resonance value throughout the mixing period, the rf field magnitude is ramped such that the sum of the effective field magnitudes passes through resonance. This imposes a time dependence on the recoupled dipolar Hamiltonian, illustrated in Figure 2B (an acceptable description when the changes in the effective fields are small over the time scale of a single rotor cycle, so that the average Hamiltonian calculation remains valid).[41] Performed slowly enough, and absent relaxation effects, one can achieve adiabatic polarization transfer in this manner.[42−44] For low-γ nuclear spins, and

(39) For an example illustrating transverse experiments in weakly coupled systems see: Verdegem, P. J. E.; Helmle, M.; Lugtenburg, J.; de Groot, H. J. M. *J. Am. Chem. Soc.* **1997**, *119*, 169−174.

(40) VanderHart, D. L.; Earl, W. L.; Garroway, A. N. *J. Magn. Reson.* **1981**, *44*, 361−401.

(41) Zhang, S.; Czekaj, C. L.; Ford, W. T. *J. Magn. Reson. A* **1994**, *111*, 87−92.

(42) Pines, A.; Gibby, M. G.; Waugh, J. S. *J. Chem. Phys.* **1973**, *59*, 569.

especially the weakly coupled spin pairs considered here, relaxation effects and limitations on mixing time due, for instance, to HPPD heating effects, make such experiments difficult or impossible.

Nevertheless, ramping the rf field such that the system passes through resonance can still provide several benefits in these cases. First, we expect almost identical manipulation of the recoupled dipolar Hamiltonian for spin pairs with slightly different resonance conditions (due to CSD and rf inhomogeneity) when the ramp starts far to one side of the resonance condition and proceeds far to the other. This implies that the spin dynamics induced by the ramping process will have significantly reduced dependence on these variables. Two factors that might affect the validity of this statement are the width of the rf distribution relative to the overall ramp width and the arc over which the effective fields move in passing through the CSD-broadened resonance condition. With respect to the first point, we note that the rf contribution to the effective field strength is small in these experiments. Hence, the width in the distribution of effective field strengths due to rf inhomogeneity is only a fraction of what it would be were the effective fields dominated by rf, as in a CP or HORROR experiment. The rf contribution to the resonance width is calculated according to

$$\Delta\omega_\Sigma \approx \Delta\omega_1\left(\frac{4\omega_1}{\omega_\Sigma}\right) \tag{12}$$

for a symmetrically placed carrier frequency. Underlying the second point is the effective-field orientation dependence of the magnitude of the recoupled interaction, so that the ratio of the CSD width of the resonances to the effective fields becomes relevant. For most systems these are minor effects and, as we demonstrate below, can be ignored.

The second and more subtle benefit that ramping affords is connected with the dependence of the exchange process on relaxation. Ramp-induced dynamics are clearly sensitive to relaxation: in its absence, polarization transfer efficiencies approaching 100% are possible by quasi-adiabatic manipulation of the system, while with fast relaxation of 2-quantum coherence, the polarization transfer efficiency is limited to 50%. However, in the "fast-passage" regime, where one ramps through the resonance condition much more quickly than required for adiabaticity, one finds (as we show below) that the induced dynamics are less sensitive to this type of relaxation. A possible rationale for this behavior is as follows. The shape of the dipolar resonance condition for a typical longitudinal exchange experiment—that is, the amount of exchange obtained as a function of mismatch from resonance for a fixed mixing time—has a characteristic dependence on the 2-quantum relaxation rate (Figure 3). With fast 2-quantum relaxation, more rapid off-resonance magnetization exchange and reduced on-resonance exchange is observed as compared to the slow 2-quantum relaxation case. If we imagine fast passage through such a resonance condition as simply summing the rates of exchange at each point along the resonance, then changes in the 2-quantum relaxation rate will not strongly influence the overall amount of exchange observed upon passing through resonance because of the compensating effects of on- and off-resonance dynamics.

We have chosen here to linearly ramp the rf magnitude ($d\omega_1/dt$ = constant), which leads to a linear response of the effective field strengths when the ramp range is small relative to their magnitudes. For linearly changing effective field strengths, the angular velocity of the Hamiltonian within *J*-space has a Lorentzian distribution (as a function of resonance mismatch), peaked on-resonance where the magnitude of the Hamiltonian is minimized. The maximum in the Hamiltonian rotation rate, particularly at this point in the sweep, reduces polarization transfer efficiency. Nonlinear rf manipulations have broader angular velocity distributions and may yield more polarization transfer for a given mixing time. Hediger *et al.*, have proposed shapes of the effective field manipulation, in the context of heteronuclear CP, which impart approximately constant angular velocity to the Hamiltonian during the sweep.[44] However, changes in the ramp rate during mixing may not be consistent with the requirements of experiments aimed at inducing identical manipulations for all spin pairs within a broadened resonance condition so that the effect of the broadening on the spin dynamics is minimized. Although some modification of the basic linear ramp may improve the overall efficiency of these experiments without reintroducing broadening-dependent effects, we have chosen to use linear ramps in these initial experiments because of their simplicity and effectiveness (demonstrated below).

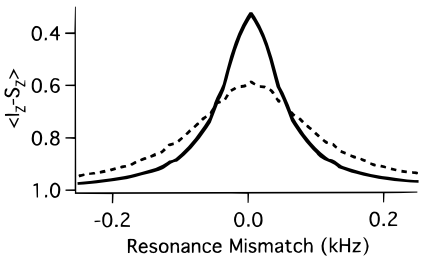

Figure 3. Simulations of magnetization exchange as a function of resonance mismatch with 2-quantum relaxation rates of 200 (solid line) and 500 (dashed line) Hz, otherwise using the parameters for TEE described in the text. On-resonance, a faster 2-quantum relaxation rate reduces exchange, while sufficiently off-resonance it increases exchange. Rapidly ramping through the resonance may reduce the dependence of the dynamics on the 2-quantum relaxation rate because of the compensating nature of this effect.

Results and Discussion

The Dipolar Resonance Condition in TEE. Figure 4A illustrates the ^{13}C chemical shift spectrum obtained from $^{13}C_2$-labeled TEE spinning at 9.900 kHz. From the molecular structure determined by X-ray crystallography,[45] the intramolecular distance between the labeled sites (4′-OH carbon of the tyrosine ring and methylene carbon of the ethyl moiety) is calculated as 5.05 Å, yielding a dipolar coupling constant of 59 Hz. The CSA tensors of the two sites, obtained from sideband patterns in slow-spinning spectra,[30] are as follows: $\delta = -7.19$ kHz and $\eta = 0.91$ for the 4′-OH carbon; $\delta = -3.20$ kHz and $\eta = 0.05$ for the methylene. The chemical shift difference is 9.410 kHz, so that a 1.54 kHz rf field (carrier precisely in the middle of the two peaks) is necessary to increase the effective field strengths to match resonance. The effective field orientations under these conditions are illustrated in Figure 4B. Note that the presence of side bands in the spectrum indicates that relative tensor orientation (CSA and dipole) will have an effect on the dipole-driven exchange dynamics (although minor as indicated by the small size of the side bands). An identical effect has been noted in $n = 1$ R^2 experiments on this compound[15] and is not introduced by the R^2T modification. The

(43) Chingas, G. C.; Garroway, A. N.; Monitz, W. B.; Bertrand, R. D. *J. Am. Chem. Soc.* **1980**, *102*, 2526.

(44) Hediger, S.; Meier, B. H.; Kurur, N. D.; Bodenhausen, G.; Ernst, R. R. *Chem. Phys. Lett.* **1994**, *223*, 283−288.

(45) Pieret, P. A.; Durant, F.; Griffe, M.; Germain, G.; Dehaerdemacker, T. *Acta Crystallogr.* **1970**, *B26*, 2117−2124.

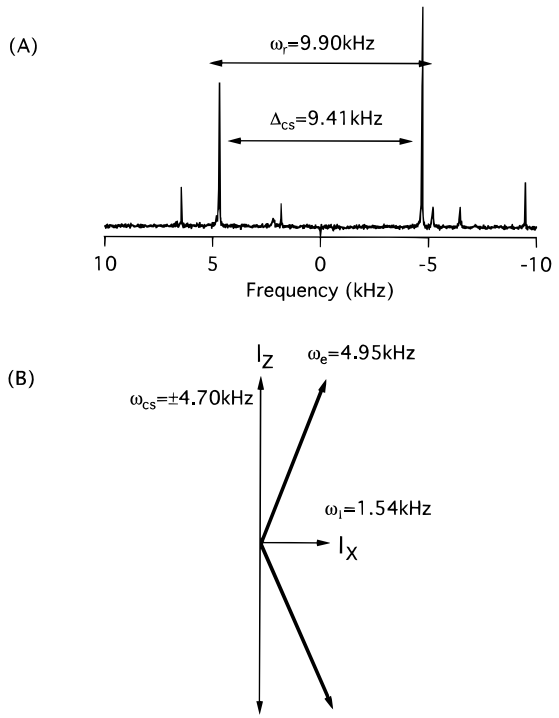

Figure 4. (A) Spectrum of $^{13}C_2$-labeled TEE, indicating the chemical shift difference between the labeled sites and the MAS frequency at which the tickling experiments were performed. (B) Effective field orientations when rf of the appropriate magnitude to induce dipolar resonance (≈1.5 kHz) is applied.

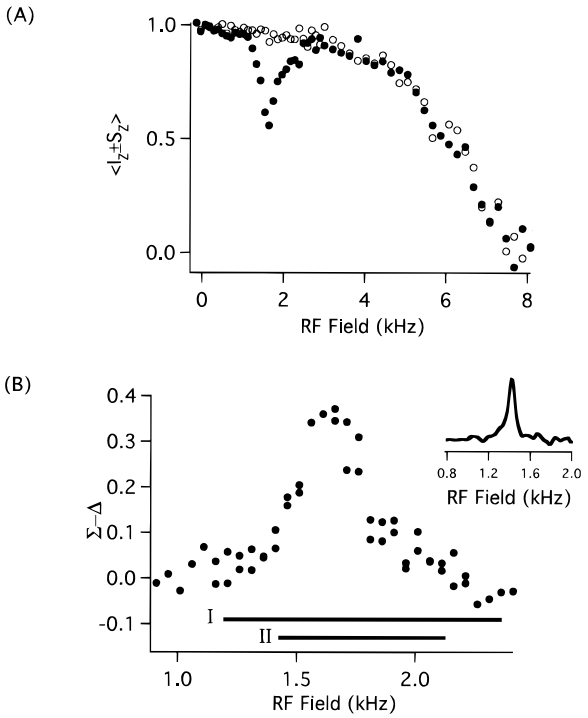

Figure 5. (A) Residual sum (open circles) and difference (filled circles) polarization after mixing for 100 ms at the indicated rf field strength. The selective decay of difference polarization near 2 kHz indicates the dipolar recoupling effect, while the simultaneous and more drastic decay of sum and difference polarization at higher field strengths is primarily caused by recoupled CSA interactions. (B) Subtraction of difference from sum polarization provides a direct look at the resonance condition. The lines under the resonance condition illustrate the ramp ranges for subsequent experiments. (Data in (A) and (B) collected in different experiments.) The inset shows the rf distribution within the coil at a typical rf field strength.

orientation of aromatic tensors in the molecular frame is known,[46] and the axial symmetry of the methylene carbon CSA makes the assignment of its orientation in the molecular frame relatively clear (symmetry axis along the C−O ester bond[15]). The relative tensor orientations were calculated using these tensor assignments and the X-ray coordinates and are described by the Euler angles (according to Spiess's convention[38]): dipolar tensor (α, β, γ) = (0°, 0°, 0°); 4′-OH tensor (0°, 55°, 37°); methylene tensor (0°, 66°, −136°).

The dipolar resonance condition was mapped out using the R^2T pulse sequence with a fixed mixing time (100 ms, with a decoupling field of 56 kHz). Sum and difference polarizations were prepared along the effective fields in separate experiments, and mixing was performed at a series of constant field strengths. The residual sum and difference polarization after each experiment is plotted in Figure 5A. Both these and subsequent data points are corrected for natural abundance background signal by a 10% subtraction ($x \Rightarrow (x - 0.1)/0.9$, where x represents data normalized so that the first point (zero mixing time) has unit intensity). The selective decay of difference polarization at an rf field strength near 2 kHz indicates the expected dipolar recoupling effect, with zero-quantum character relative to the rotating frame. The simultaneous and more substantial decay of sum and difference polarization at larger field strengths is primarily due to CSA recoupling as each effective field approaches the spinning speed.[47−49] Although a component of the dipolar coupling is also recoupled at this condition, its effects are overshadowed by the recoupled CSA interactions. Experiments with asymmetric carrier placement can allow access to this recoupling condition without CSA recoupling, for a variety of effects.

Subtracting difference from sum polarization permits a more detailed examination of the resonance shape (Figure 5B). The shape is approximately centered about the expected rf magnitude of 1.54 kHz, although with a slight upfield shift that may be due to the long low-field tail of the rf distribution (upfield shifts in the resonance condition can also come from components of the CSA interaction that are perpendicular to the effective fields,[28] but this effect is expected to be minor here). The width derives from several factors including rf inhomogeneity, chemical shift dispersion, and the natural width of the exchange process (dependent on the size of the dipolar coupling constant and the 2-quantum relaxation rate). The inset shows the rf distribution obtained at an intermediate rf field strength (1.45 kHz). The width of the rf distribution at half-height (0.1 kHz) is approximately 7% of the center value, although with a significant low-field tail. The lines under the resonance indicate the range of two ramps used in subsequent experiments (ramp I 2.35−1.20 kHz; ramp II 2.15−1.45; these correspond to effective field ramp widths on the order of 0.2−0.35 kHz).

R^2T vs $n = 1$ R^2 Spin Dynamics in TEE. Ramping through the resonance condition at a series of rates yields the exchange curves shown in Figure 6. In Figure 6A, the decay of difference polarization is plotted as a function of mixing time in experiments where ramp I (range indicated in Figure 5B) was used. Control experiments using sum polarization show no detectable decay (±5%), even at modest ^{1}H decoupling power (56 kHz). In Figure 6B, difference polarization is plotted as a function of the rf ramp rate (ramp width divided by mixing time) to allow comparison of data obtained using different ramp ranges. Data from experiments using both of the ramps indicated in Figure

(46) Veeman, W. S. *Prog. NMR Spectrosc.* **1984**, *16*, 193−235.
(47) Gan, Z.; Grant, D. M. *Chem. Phys. Lett.* **1990**, *168*, 304.
(48) Gan, Z.; Grant, D. M.; Ernst, R. R. *Chem. Phys. Lett.* **1996**, *254*, 349−357.
(49) Sun, B.-Q., unpublished results.

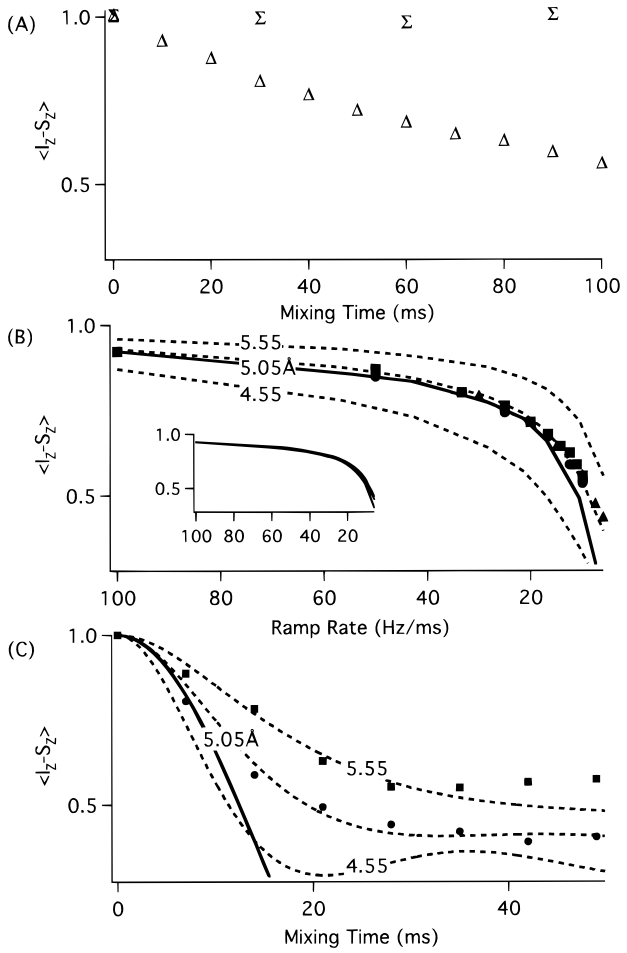

Figure 6. (A) Decay of sum (Σ) and difference (Δ) polarization as a function of mixing time for R^2T experiments on $^{13}C_2$-labeled TEE using ramp I and a ^1H decoupling power of 56 kHz. (B) Decay of difference polarization plotted as a function of ramp rate for ramp I (squares, ^1H decoupling power of 56 kHz during mixing; circles, 76 kHz) and ramp II (triangles, 56 kHz). The inset indicates the variation in exchange curves expected for a large variation in 2-quantum relaxation rate with the distance held constant (see text). (C) Decay of difference polarization as a function of mixing time for $n = 1$, on-resonance R^2 experiments on the same sample (squares, 56 kHz ^1H decoupling; circles, 76 kHz). Simulations (solid and dashed lines) are described in the text.

5B and with 56 kHz decoupling power approximately overlap, demonstrating that the technique is not sensitive to the details of the ramp when plotted in this manner. Furthermore, repeating the experiment with ramp I and a significantly higher decoupling power during mixing (76 kHz) also yields overlapping data. Hence the experiment appears to be insensitive to the change in the 2-quantum relaxation rate induced by the change in decoupling power (demonstrated below). Simulation of the expected dynamics using a dipolar coupling constant corresponding to the known internuclear distance yields the solid line in the plot. Simulations that include a 0.1 kHz relaxation rate for 2-quantum coherence (estimated from single-quantum homogeneous linewidth measurements using a single-π pulse Hahn echo sequence), and performed for the indicated series of internuclear distances, yield the dashed curves, with the 5.05 Å curve matching the experimental data quite well. Three points are important: first, the deviation from ideal coherent dynamics is quite small compared to other techniques (see below) and is fully accounted for by inclusion of zero-quantum relaxation in the simulation. Second, the particular value selected for the zero-quantum relaxation rate does not strongly affect the results, as indicated both by the insensitivity of the experiment to decoupling power and to the fact that calculations using relaxation rates differing by a factor of 2 in either direction do not yield significantly different exchange curves. The inset in Figure 6B shows simulated curves using a distance of 5.05 Å and 2-quantum relaxation rates of 0.05, 0.1, and 0.2 kHz. Third, the dynamics remain a strong function of the dipolar coupling constant and hence allow accurate extraction of the internuclear distance primarily as a single-parameter fit.

Figure 6C shows the on-resonance, $n = 1$ R^2 exchange dynamics for comparison (exchange curve acquired using the R^2T pulse sequence with no rf during dipolar mixing and RI and RO pulses omitted). Data were acquired at both decoupling powers (56 and 76 kHz), and the two curves differ markedly. This confirms the expected change in the 2-quantum relaxation rate with the indicated change in decoupling power. A simulation of the dynamics ignoring relaxation and CSD effects, and using a 59 Hz coupling, yields the solid line in the plot. Simulations that include estimates of 2-quantum relaxation and the width of the inhomogeneously-broadened resonance condition (≈40 Hz) are shown for the indicated range of internuclear distances (dashed lines). Both corrections to the "ideal" simulation are needed to approximate the experimental data, and the magnitude of the correction is much larger than for the equivalent R^2T experiment. These additional parameters must be accurately estimated to calculate the appropriate exchange curve, and hence allow extraction of the internuclear distance.

R^2T Spin Dynamics in GG-HCl. The R^2T experiments were repeated for $^{13}C_2$-labeled GG-HCl. The N-terminal α and terminal carboxyl carbons are labeled, with an intramolecular distance according to the neutron diffraction structure of 4.56 Å.[50] Even diluted 1:10, however, a detailed series of RFDR experiments has shown that intermolecular interactions lead to an effective dipolar coupling constant of approximately 95 Hz (corresponding to an effective internuclear distance of 4.3 Å), rather than the 80 Hz coupling expected.[12] The CSA tensor elements are as follows: $\delta = -9.1$ kHz and $\eta = 0.75$ for the carboxyl carbon; $\delta = -1.5$ kHz and $\eta = 0.99$ for the α-carbon. The chemical shift difference is 12.880 kHz, so that at a spinning speed of 13.200 kHz an rf field strength of 1.44 kHz is required to induce resonance. Because the spinning speed greatly exceeded the magnitudes of the CSA tensors, the relative tensor orientations were ignored. Figure 7A illustrates the dipolar resonance condition mapped out for this sample under the given conditions (with a 100 ms mixing time and 80 kHz decoupling power), and the lines under the resonance indicate the ramp ranges used for subsequent experiments.

Ramping through the resonance condition using ramp I yields the time course for sum and difference polarization shown in Figure 7B. Both difference and sum polarization decay as a function of mixing time, the difference between the two demonstrating a zero-quantum dipole-driven effect. The decay of sum polarization (approximately 10% over 100 ms) is not due to the recoupled dipolar interaction because of the latter's zero-quantum form (although for more strongly coupled pairs, and particularly in the presence of ^1H nuclei, higher-order dipole-dependent effects can occur). The decay may instead be due to several processes including $T_{1\rho}$ relaxation and probe heating effects. Signal losses of this type, which affect each spin independent of the coupling between them, must be taken into account in analyzing the decay of difference polarization. As long as the effects are on a significantly slower time scale than 2-quantum relaxation, they can be compensated for by dividing the residual difference polarization by the residual sum polarization for each mixing time. The procedure is similar to the S/S_o

(50) Koetzle, T. F.; Hamilton, W. C. *Acta Crystallogr.* **1972**, *B28*, 2083.

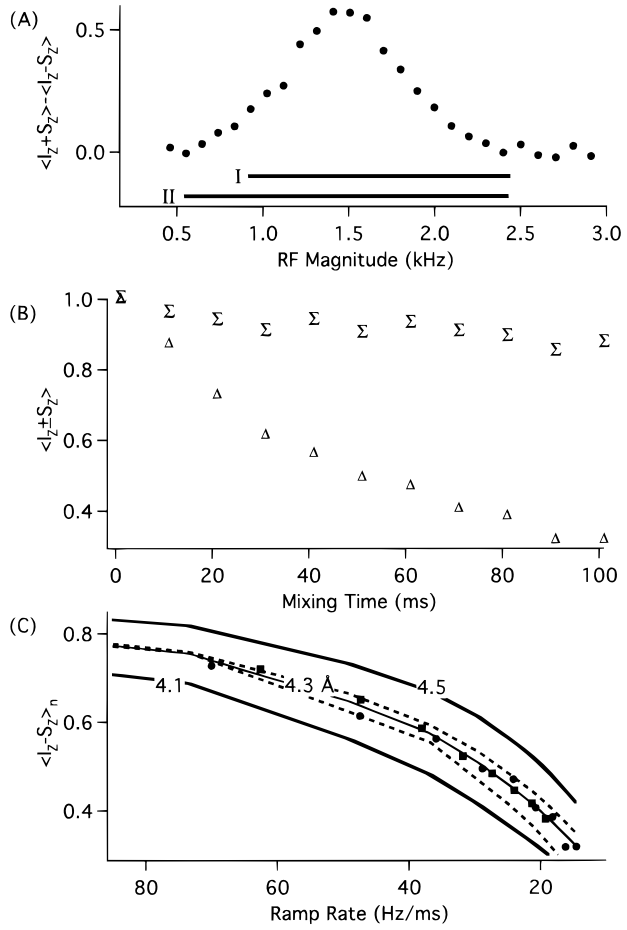

Figure 7. (A) Dipolar resonance condition for $^{13}C_2$-labeled glycyl-glycine hydrochloride under conditions described in the text. The lines under the resonance indicate ramp ranges. (B) The decay of sum (Σ) and difference (Δ) polarization as a function of mixing time for R^2T experiments performed using ramp I at 80 kHz ^{1}H decoupling. (C) The decay of "normalized" difference polarization as a function of ramp rate for data obtained using ramp I (circles) and ramp II (squares). Simulations (solid and dashed lines) are described in the text.

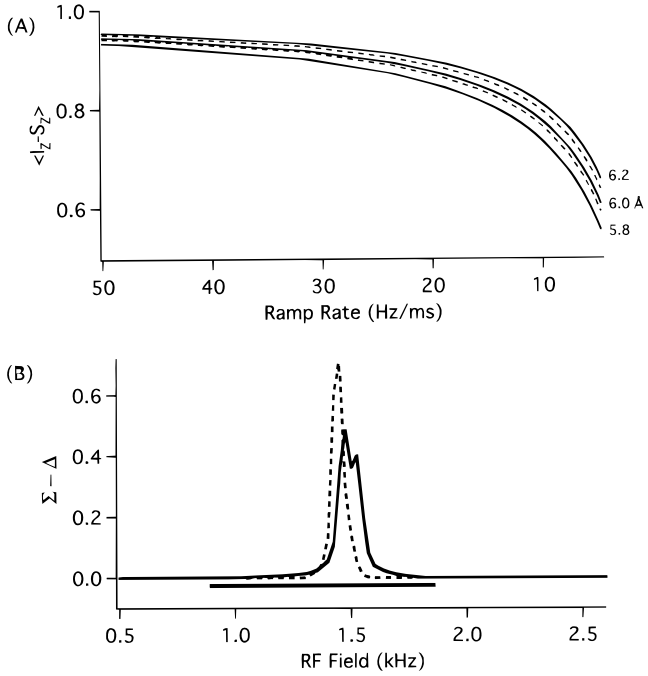

Figure 8. (A) Simulated decay of longitudinal difference polarization for $^{13}C_2$ internuclear distances of 5.8−6.2 Å (solid lines) spin system parameters appropriate for the GG-HCl sample described in the text (2-quantum relaxation time set to 3.5 ms). Simulations in which the distance is fixed (6.0 Å) and the 2-quantum relaxation time is varied (2 and 5 ms) are indicated by dashed lines. (B) Simulated resonance condition for a $^{13}C_2$ 6.0 Å distance and GG-HCl spin system parameters, with (solid line) and without (dashed line) CSA effects included. The CSA-induced broadening of the dipolar resonance condition is similar to the well-known Bloch−Siegert shift.

normalization common in heteronuclear REDOR experiments;[51] however, the correction is expected to be much smaller in most R^2T experiments reflecting the slower decay of the control curve relative to dipole-driven evolution. Here we have used an exponential fit to the sum polarization decay curve ($T_{1\rho} = 640$ ms), rather than the sum curve itself, to correct the difference decay curve.

Figure 7C shows the decay of normalized difference polarization as a function of ramp rate for both ramp ranges. The data from the two ramps overlap and match the appropriate simulated curve (solid lines calculated with dipolar coupling constants corresponding to the indicated distances and a 3 ms 2-quantum relaxation time). Additional simulations using a 4.3 Å distance and varied 2-quantum relaxation times (2 and 5 ms) are indicated by dashed lines. The divergence between these simulations grows with decreasing ramp rate, indicating the increase in sensitivity of the exchange curve to the 2-quantum relaxation rate for slower-passage experiments. Even at the slowest ramp rates shown here, however, the uncertainty in the distance measurement that would arise from a large uncertainty in the value of the zero-quantum relaxation time is less than 0.1 Å.

Outer Range of R^2T Distance Measurements. Accurate R^2T distance measurements can be made when (i) an easily detectable amount of magnetization exchange occurs and (ii) the exchange trajectory remains relatively independent of variables other than the dipolar coupling constant, particularly the rate of 2-quantum relaxation. In Figure 8A, we plot (solid lines) the decay of difference polarization as a function of ramp rate expected for ^{13}C spin pairs separated by 5.8, 6.0, and 6.2 Å. The simulation parameters are otherwise identical to those for GG-HCl reported above and assume a 2-quantum relaxation time of 3.5 ms. Keeping the distance at 6.0 Å and using relaxation times of 2 and 5 ms yields the dashed curves. Comparison of the two sets of curves indicates that relative insensitivity to 2-quantum relaxation is maintained at least out to 6 Å distances.

Achieving reasonable levels of exchange (which we roughly define as $\langle I_z - S_z \rangle$ values <0.7−0.8) for a spin pair separated by 6 Å requires ramp rates approaching 5 Hz/ms. This is slightly slower than the slowest ramp rates reported here (7 Hz/ms for TEE) and requires either a narrower ramp range or longer mixing times. Based on the measurements here, overall signal loss during mixing should be small (<20%) even for mixing times approaching 200 ms, so that the length of the longest accessible mixing time will depend primarily on probe performance limitations at low to moderate ^{1}H decoupling field strengths. Narrower ramp ranges are also in principle possible. Figure (8B) plots the simulated resonance condition for the 6 Å spin pair with (solid line) and without (dashed line) CSA interactions included in the calculation. The intrinsic width of the resonance condition in the absence of CSA interactions is determined by the magnitude of the recoupled dipolar interaction and for 5−6 Å $^{13}C_2$ distances is under 100 Hz. When CSA interactions of sufficient magnitude are present, the (spin) components of the CSA that are perpendicular to the effective fields induce a Bloch−Siegert-like shift and broadening of the dipolar resonance[28] that increases the width to 100−200 Hz.

(51) Gullion, T.; Schaefer, J. *J. Magn. Reson.* **1989**, *81*, 196.

This is still much narrower than the 0.7−2 kHz ramp ranges used in the experiments detailed here and leaves room for broadening from both CSD and rf inhomogeneity. Given mixing times of 10−200 ms and the 1 kHz ramp indicated in Figure 8B, the entire range of ramp rates in Figure (8A) is accessible. Hence, under moderately favorable conditions, accurate distance measurements out to at least 6 Å should be possible.

Conclusions

Although a wide variety of theoretical solutions have been presented for the dipolar recoupling problem in solids, in practice many have proven to be of limited utility for extracting accurate distance information over structurally useful distance ranges because of limitations in probe performance (e.g., accessible ^{1}H decoupling power over significant mixing times and rf stability). The ramped-R^{2}T technique described here, although limited to homonuclear spin pairs with well-separated chemical shifts, will allow accurate distance measurements over relatively long ranges (e.g., out to 5−6 Å for ^{13}C pairs, with an accuracy expected to be on the order of 0.1 Å when S/N is not the limiting factor). The experiment is effective without placing stringent demands on probe decoupling performance, without significant signal loss during mixing, and without the need to include a series of difficult-to-define spin system parameters in the simulation process. We have demonstrated these properties on a pair of model compounds containing spin pairs with intramolecular distances of 4.5−5 Å.

Furthermore, the ramped techniques we have described for accurate distance measurements in weakly coupled systems should be equally applicable to the related resonance experiments heteronuclear CP (under fast spinning conditions) and HORROR. In the former case, this suggests a method for extracting heteronuclear distance information (e.g., ^{13}C/^{15}N) and, in the latter case, for measuring accurate distances for homonuclear spin pairs with small chemical shift differences. Finally, the R^{2}T technique may be particularly useful when applied to uniformly labeled compounds within the framework of a two-dimensional correlation experiment. Ramping the rf field over sufficient range to pass through a series of resonance conditions corresponding to different spin pairs within the sample would yield recoupling over a selected region of the spectrum. Each spin pair, recoupled in turn during the ramping process, is recoupled with near-R^{2} chemical shift selectivity. This may allow extraction of distance information between weakly coupled spin pairs in these samples where broad-band recoupling would lead to a strongly coupled spin matrix whose dynamics are approximately independent of the weaker couplings.

Acknowledgment. We thank Chad Rienstra for design and construction of the transmission-line probe used in these experiments, and Dennis Hall, John Gross, and Dr. Joanna Long for enlightening discussions. This work was supported by grants from the National Institutes of Health (GM-23403, NS-33366, RR-00995).

JA964313Z